Fourth International Symposium on Marine Propulsors
smp'15, Austin, Texas, USA, June 2015

Prediction of Steady Performance of Contra-Rotating Propellers with Rudder

Yasuhiko Inukai[1], Takashi Kanemaru[2], Jun Ando[2]

[1] Japan Marine United Inc.,Tokyo, Japan
[2] Kyushu University,Fukuoka, Japan

ABSTRACT

To reduce fuel oil costs and emission of greenhouse gases of ships in operation, application of Contra-Rotating Propellers (CRP) will be one of the solutions, which have high propulsive efficiency. The prediction of CRP performance is more difficult than that of a conventional single propeller because the aft and forward propeller interact each other strongly. Moreover, an existence of a rudder changes the power balance between the aft and forward propeller. To solve the interaction between two propellers and a rudder correctly is key to successful design of CRP. Although many performance prediction methods of CRP have been developed until now, most of them use a simplified model regarding to a trailing wake deformation and geometries of a propeller and a rudder. Recently, the authors have developed a prediction method of steady performance of CRP without a rudder, in which we treat trailing wake deformation rigorously by using a simple surface panel method "SQCM". For further improvement as a design tool for CRP, we include an influence of a rudder, represented by source distributions on the surface and discrete vortex distributions arranged on the mean camber surface according to QCM (Quasi-Continuous vortex lattice Method), in the method. To verify the present method, we carried out open water tests for CRP combined with a rudder and sea trial with varying the horsepower ratio between aft and forward propeller. The present method shows good agreements with the experiments and we confirm its validity.

Keywords

Conta-Rotating Propellers, SQCM, Rudder.

1 INTRODUCTION

Contra-rotating propellers (CRP) is well known and promising technology as one of the most efficient propulsion. The high performance has been shown in many reports (e.g. Inukai. 2011, Nishiyama et al. 1990). The number of the application is expected to increase in the circumstance that energy saving technologies draw much more attention than ever since EEDI entered into force in 2013. In order to apply CRP successfully to various kinds of vessels, a sophisticated performance prediction method is necessary.

While a number of researches have been done for predicting characteristics of CRP, those considering an effect of a rudder are few. It is well known that a rudder influences much on the characteristics of CRP (Sasaki. 1990). The difference of the wake fraction of the rudder between the aft and forward propeller changes the power balance among two propellers. And a rudder resistance increases than that of a conventional single propeller because there is less rotational flow in the propeller slipstream. Sasaki (1990) presented a design method for CRP, including an effect of a rudder based on a simplified theory by representing a propeller as infinite blade disk and a rudder as a rectangular plane on which sources and vortices are distributed. He verified the effectiveness of the method by comparing calculation to self-propulsion tests. Although his method is good for understanding an effect of a rudder on CRP, it is too simple for practical design because accurate geometry of propeller and rudder cannot be treated.

The authors (2014) have recently developed a steady performance prediction method of CRP based on a simplified surface panel method "SQCM" (Ando. 1995) with fully wake alignment. Subsequently, we undertook a development of a steady performance prediction method of CRP with an effect of a rudder. A rudder is represented a rudder as source distributions on the rudder surface and discrete vortex distributions arranged on the mean camber surface as well as a propeller. To verify the accuracy of the present method, open water tests with rudder were carried out. Then, in the sea trials of vessels with CRP, we changes the propeller speed ratios between the aft and forward propeller and measured how the power balances between the aft and forward propeller changed.

In this paper, an outline of the present method is described at first. Then, we compare the calculation with experiments and discuss the comparison results.

2 CALCULATION METHOD

The "SQCM" (Source and Quasi-Continuous vortex lattice Method) is a simplified surface panel method developed at Kyushu University. This method uses source distributions (Hess et al. 1964) on the blade surface and discrete vortex distributions arranged on the mean camber surface according to QCM (Quasi-Continuous vortex lattice Method) (Lan. 1974). Figure 1 shows an illustration of the arrangement of the singularities. These singularities should satisfy the boundary condition that the normal velocity is zero on the blade and mean camber surfaces. The control points of the vortex are placed at the trailing edge to prevent the flow normal to the camber surface at the trailing edge. By doing so, Kutta condition can be satisfied without iterative calculation. The singularities on a rudder are arranged in a same manner as those on a propeller blade. A trailing wake of a propeller is deformed non-linearly in accordance with a direction of local flow until two and a half rotations. The local velocities are calculated at the calculation points, which are arranged at the center of lattices of the wake sheet, and interpolated at the nodes of the lattices. For more detailed procedures, see the reference (Inukai et al. 2014). The pitch of the wake sheet after two and half rotations is simply assumed the same as the geometric pitch because the viscosity influenced much on the trailing wake away from the blade and the geometry estimated by the inviscid wake model adopted in the present method becomes different from the actual one. While the trailing wake of rudder, of which length is five times the chord length, is fixed because of the simplicity. Figure 2 shows an illustration of the panels of the trailing wake and the surfaces of propellers and rudder.

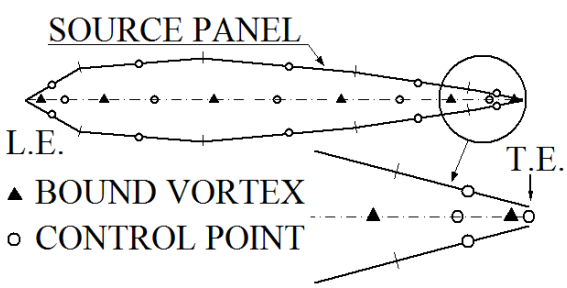

Figure 1: Arrangement of source panels, bound vortices and control points in SQCM. (Ando et al. 1995)

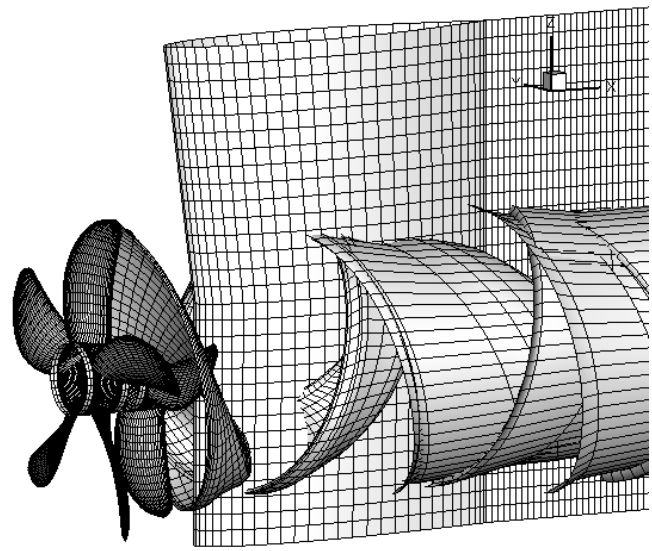

Figure 2: Panels of trailing wake and surfaces of propellers and rudder.

The interaction between propellers and a rudder is inherently unsteady. However, our concern is time-averaged characteristics of CRP and rudder. Thus, we treat the interaction as a steady problem by taking the mean value of each induced velocities in the circumferential direction. The induced velocities to propellers are calculated on the mid chord line and those to a rudder are calculated at the midpoint of every panel of the rudder surface and the mean camber surface. Figure 3 shows a calculation flow chart. Iterative calculations continue until the convergence of the total thrust of the propeller and rudder is obtained. In the calculation, the following assumptions are made.

1. The trailing wake of propellers penetrates other propeller and rudder. Meanwhile, the induced velocity of the vortex inside the rudder is omitted.

2. The frictional resistance of the rudder R_{FRUD} is calculated using the drag coefficients by the formula (1) (ITTC. 2008). The drag coefficient and lift gradient correction factor of the propeller is determined using a regression equation from our tank test database.

$$R_{FRUD} = 0.5(1 + 2\delta + 60\delta^4)C_F\rho V^2 S, \qquad (1)$$

Where, δ is the maximum thickness ratio, ρ is the density, V is the chordwise averaged velocity, S is the wetted surface area of the chordwise stripe and C_F is calculated according to the following equations.

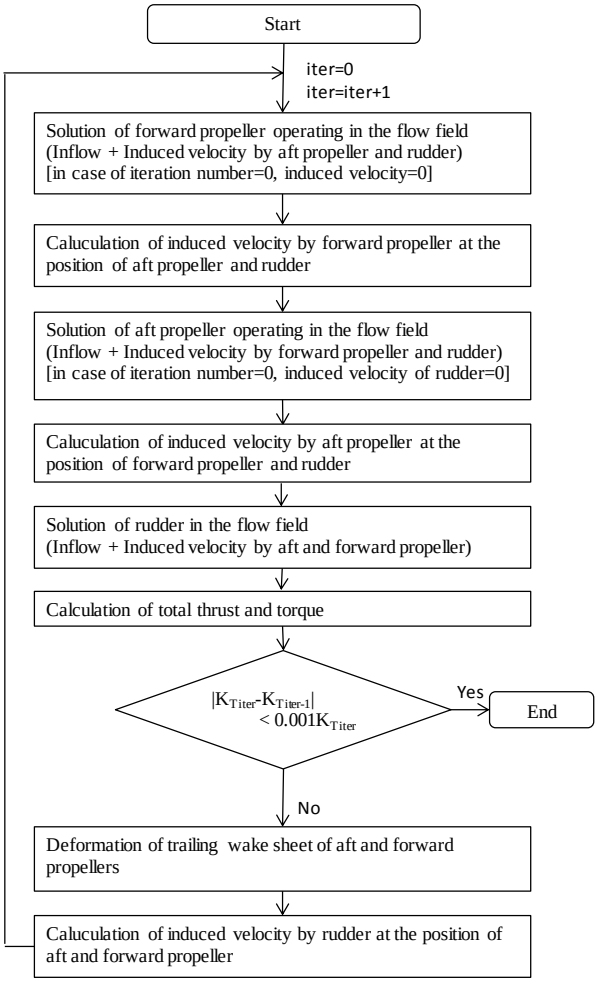

Figure 3: Calculation flow chart.

For outer zone of propeller slip stream

$$C_F = \frac{1.327}{R_e^{0.5}} \text{ for Re} < 5.25\times10^4$$

$$C_F = C_F^* 10^{0.117 f(Re)} \text{ for } 5.25\times10^4 < \text{Re} < 2.0\times10^6$$

$$C_F = \frac{1}{(3.46 log_{10} Re - 5.6)^2} - \frac{1700}{Re} \text{ for } 2.0\times10^6 < \text{Re}, \quad (2)$$

where,

$$C_F^* = \frac{1}{(3.46 log_{10}(2*10^6 - 5.6)^2} - \frac{1700}{2*10^6}$$

$$f(Re) = \{log_{10} Re - log_{10}(2*10^6)\}^2$$

Re is the Ryenolds Number.

For inner zone of propeller slip stream

$$C_F = \frac{0.075}{(log_{10} Re - 2.0)^2} \quad (3)$$

3. Bernoulli constant increases across the propeller plane. Thus the constant on the rudder surface is determined using the value of the same streamline after two rotations of forward propeller.

4. The hub vortex is not modeled. The diameter of trailing wake at the root of the propeller blades is same as the boss diameter. The flow velocity on the shaft center line is same as that of the onset flow, and that between the shaft center and the hub diameter is linearly interpolated.

5. In order to prevent divergence of the calculation, if the distance of the adjacent nodes of the trailing wake panel is greater than an allowable distance L, it is fixed to the L. The deformation at the tip is generally calculated too large, although the actual shape of wake sheet at the tip is rolled up due to an effect of viscosity. Thus, we applied 0.01 times of propeller radius, R, as the allowable distance for the propeller radius above 0.99R. For the radius below 0.99R, 0.1R were applied as the allowable distance.

3 OPEN WATER TESTS

3.1 Setup

Open water tests with and without a rudder for CRP and conventional single propeller (SP) were carried out at the Japan Marine United Yokohama towing tank of which length is 200m, width is 10m and depth is 5m. Table 1 and Table 2 show principal particulars of the propellers and rudder respectively. The same rudder was used for both CRP and SP. Figure 4 shows a setup of the experiment. As shown in Figure 4, the forces of the propellers and the rudder were measured by each dinamometer. Free surface is covered by plate to suppress the wave interference to the models. The distance between the propeller and rudder, which is represents l, was varied in 3 cases of l/D= 60.2%,65.0% and 76.9% for CRP and 55.9%,65.9% and 75.9% for SP. The l/D of CRP represents the distance between the intermediate position between aft and forward propeller and the rudder shaft, which is normalized by a diameter of the forward propeller.

Table 1: Principal dimensions of propellers.

	CRP		SP
Diameter (m)	0.21	0.18	0.21
Pitch Ratio	0.88	0.92	0.7
Number of Blades	5	4	4
Boss Ratio	0.2159	0.2509	0.18
Propeller revolution ratio of forward propeller to aft propeller nf/na	1.3		-
Shaft Center Height (m)	0.1145		0.1145
Reynolds' Number (Kempf)	2.0×10^5		2.0×10^5

Table 2: Principal dimensions of rudder.

Chord Length	(m)	top	0.2269
		bottom	0.2052
Max. Thickness	(m)	top	0.0454
		bottom	0.0295
Height from Base Line	(m)	top	0.3176
		bottom	0.0432

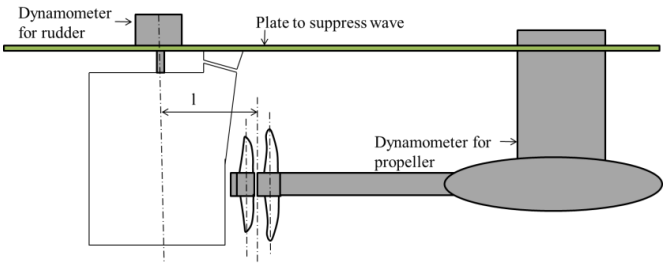

Figure 4: Setup of experiment.

3.2 Comparison between Calculation and Experiments

Figure 5 and Figure 6 show the propeller thrust coefficient K_T, propeller torque coefficient K_Q and rudder thrust coefficient K_{TRUD} without and with a rudder at l/D=65.0% for CRP and 65.9% for SP. All values of K_T, K_Q, K_{TRUD} and advance ratio J for CRP are normalized by the dimension and revolution number of a forward propeller. We can see that the calculation results agree largely well with the experiments for both without and with the rudder over whole ranges of J. Meanwhile, the K_T of the aft propeller, especially with rudder, is a little bit underestimated. In the present method, the pressure at the end face of the propeller hub is omitted. It may cause the discrepancy of K_T of the aft propeller. The hub geometry and model of hub vortex should be considered for further improvement.

Figure 7 shows the effect of the distance between the propellers and rudder on the potential wake of the rudder at J=0.6 for CRP and J=0.45for SP. The potential wake of the rudder was calculated by the toque identity method using J-K_Q curve without rudder. The calculation results agree very well with the experiments. It is found that the rudder wake to the aft propeller is larger than that to the forward propeller because the distance from the rudder is closer. And the rudder wake to CRP, i.e. in case of regarding CRP as one propulsion system, is almost same as that to SP.

Figure 8 shows the effect of distance between the propeller and rudder on the K_{TRUD}. The slope of K_{TRUD} against l/D can be well predicted, while the estimated absolute value differs a little bit from the experiment. Because the condition of the boundary layer on a rudder is complex as Moriyama et al. (1981) studied, the frictional drag coefficient used in the present method may be different from that actual value. Moreover, the correct model of hub vortex is necessary for more accurate estimation. However, we can say that the present method can estimate accurately open water characteristics of propeller with rudder for practical design purpose.

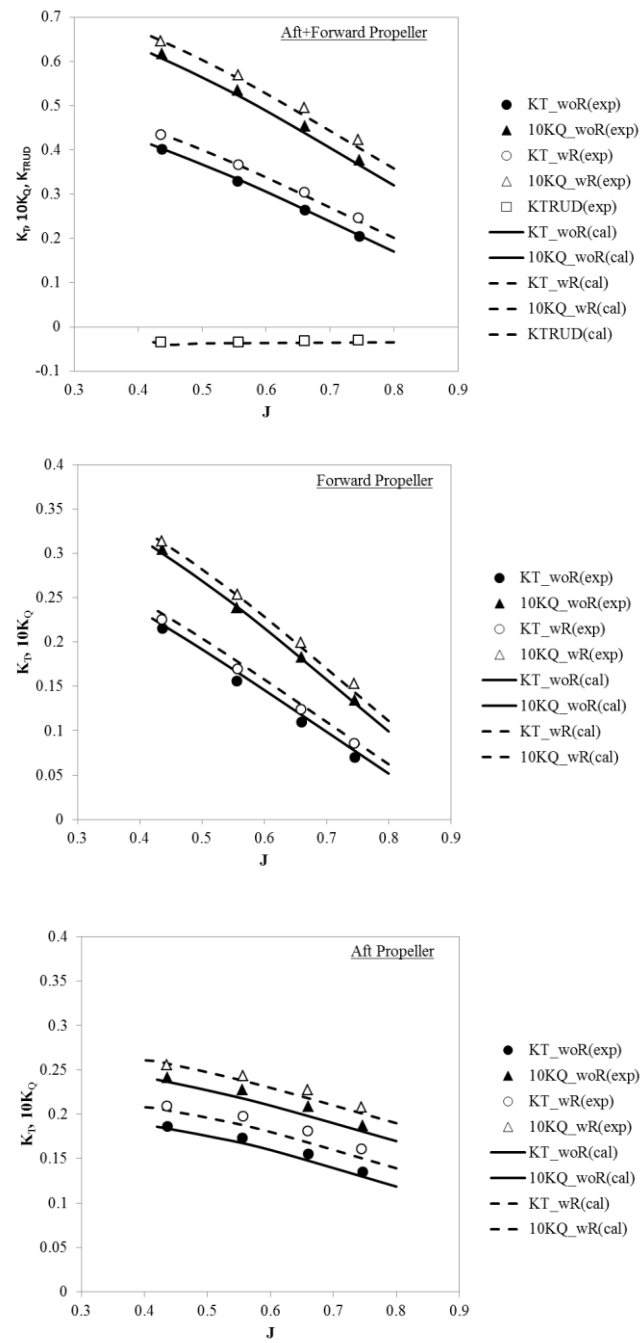

Figure 5: Open water characteristics of CRP at l/D=65.0%

Upper: Aft and forward propeller, Middle: Forward propeller, Lower: Aft propeller

(Black marks: experiment without rudder, white marks: experiment with rudder, solid lines: calculation without rudder, dotted lines: calculation with rudder)

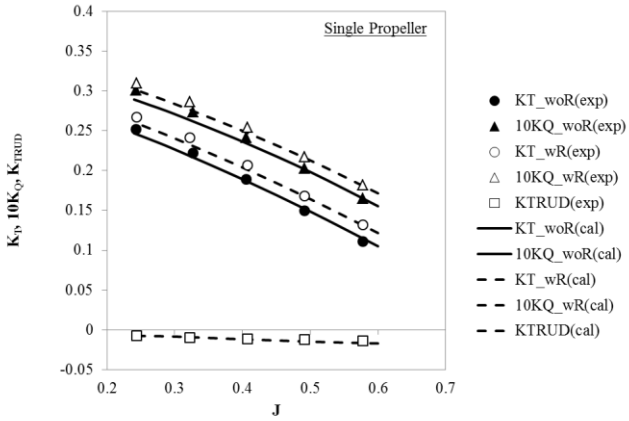

Figure 6: Open water characteristics of SP at l/D=65.9% (Black marks: experiment without rudder, white marks: experiment with rudder, solid lines: calculation without rudder, dotted lines: calculation with rudder)

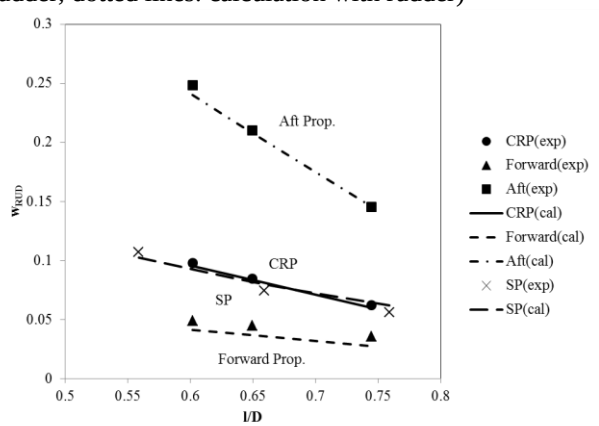

Figure 7: Effect of the distance between the propellers and rudder on the potential wake of the rudder to the propellers at J=0.6 for CRP and J=0.45for SP. (Black marks: experiment, solid lines: calculation)

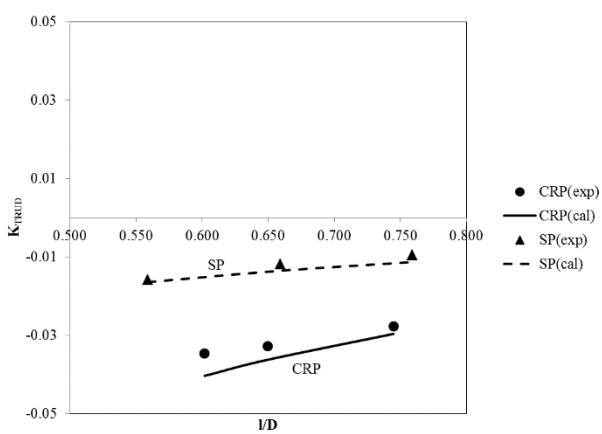

Figure 8: Effect of the distance between the propellers and rudder on the rudder thrust K_{TRUD} at J=0.6 for CRP and J=0.45for SP. (Black marks: experiment, solid lines: calculation)

4 FULL SCALE TEST

4.1 The Subjected Vessels

We carried out speed tests with varying the power ratio of the forward propeller to total power (Pf/P) for three vessels during their sea trial. These vessels are driven by a diesel electric system and the propeller revolution of aft and forward propeller can be controlled independently (Inukai. 2010). Table 3 shows the principal dimensions of the vessels. Propeller revolutions of the aft and forward propellers were varied to achieve Pf/P=0.5, 0.7 and 0.9 by keeping the same total power.

Table 3: Principal dimensions of vessels

Ship		A	B	C
Type		Tanker	Cement Carrier	Cement Carrier
Length bp	(m)	69.95	72	109
Breadth	(m)	11.5	14.6	18.2
Depth	(m)	5.25	7.6	9.4
Propulsion Motor	(kW)	600kW×2	900kW×2	1,400kW×2

4.2 Influence of hull wake on the Pf/P

Although we don't treat the influence of hull wake in the present method, it should be considered when comparing the calculation results with sea trial results. In general, aft propeller has a smaller diameter than the forward propeller and it makes the Pf/P behind hull smaller compared with that in open water. Figure 9 shows self-propulsion test results without rudder on the Pf/P compared with open water tests. The Pf/P behind the ship is averagely smaller at 2% than that in open water. Thus, the estimated Pf/P in open water were reduced 2% for an estimation of the Pf/P behind the ship.

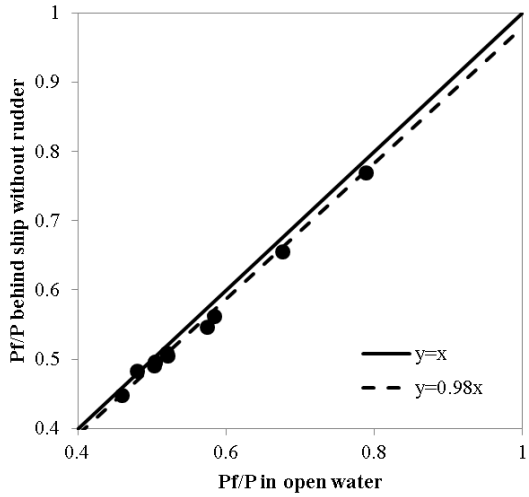

Figure 9 : Power ratio of the forward propeller to total power in .open water and behind ship without rudder.

4.3 Comparison between Calculation and Experiments

Calculations were made to estimate the Pf/P at the corresponding propeller revolutions to those in the sea trials. Figure 10 shows the Pf/P of both calculation and experiments. The working advance ratio J of the experiments was determined by the torque identity method. Figure 10 shows that the estimated Pf/P agrees very well with those of the experiments for ship B and ship C, while the present method underestimated for ship A. As to ship A, the discrepancy from the experiments becomes bigger as the Pf/P increases and the error of the prediction is 2% at the Pf/P=0.5 and 4% at the Pf/P=0.9. Although the reason why the discrepancy of the ship A is bigger than that of the other ships is not clear yet, an assumption on the effect of the hull wake on the Pf/P may be too simple. Further study on the interaction between hull and propeller is necessary.

However, from view point of a practical design, most important is to estimate accurately the power balance between aft and forward propellers at the design point, which is the Pf/P=0.5 for all vessels in this study, in order to ensure proper margins in propeller revolutions. In this sense, we can say that the present method has enough accuracy for a practical tool for CRP design.

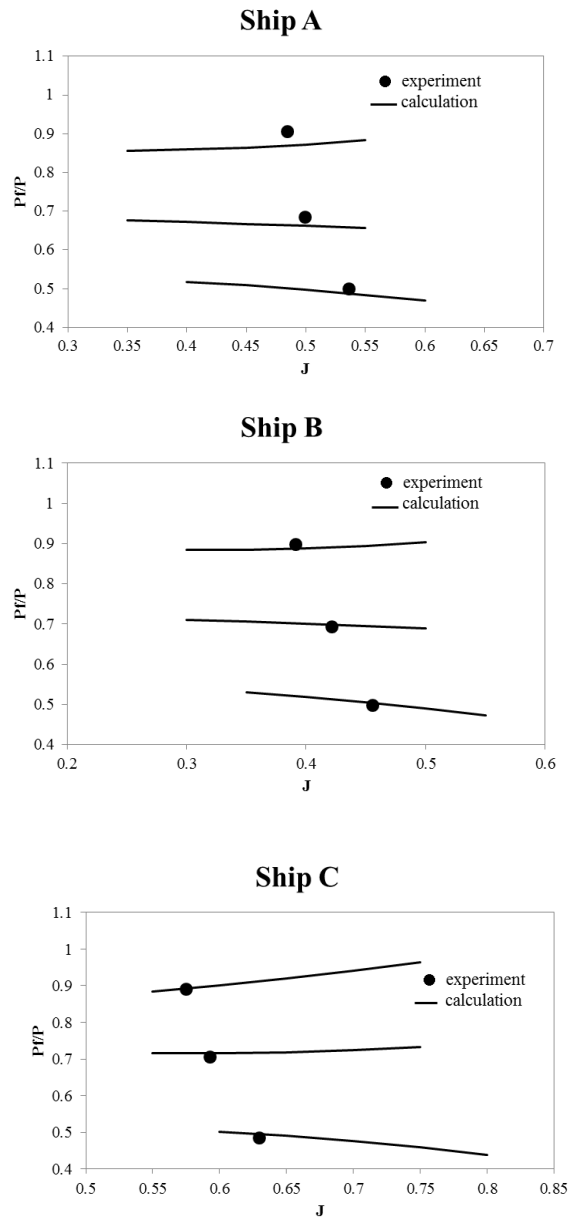

Figure 10 : Power ratio of the forward propeller to total power (Pf/P) for Ship A (upper), Ship B (middle) and Ship C (lower).

5 CONCLUSIONS AND FUTURE WORK

We developed a steady performance prediction method of CRP with an effect of a rudder. The trailing wake of the propeller is aligned in accordance with a direction of local flow. Although the interaction between propellers and a rudder is inherently unsteady, for simplicity we treat the interaction as a steady problem by taking the mean value of each induced velocities in the circumferential direction.

To verify the present method, the open water tests without and with rudder were carried out. The open water characteristics with a rudder can be well predicted by the present method. Meanwhile, the discrepancies from the experiments are shown on the rudder resistance and the thrust of the aft propeller. For further improvement, more rigorous treatment of frictional drag of the rudder and the detailed modeling of the propeller boss are necessary.

In addition to the model tests, we carried out the sea trials with varying the horsepower ratio between aft and forward propeller. Calculations were made to estimate the power ratio of the forward propeller to total power, Pf/P, at the corresponding propeller revolutions to those in the sea trials. The calculated Pf/P agreed well with those of the experiments. From the studies, the validity of the present method was confirmed.

The interaction between hull and CRP is our next question. By analyzing our database of model and full scale tests with the present method, we will investigate closely the interaction between hull and CRP, such as the effective wake fraction, and clarify the comprehensive propulsive performance of a vessel with CRP.

REFERENCES

Ando, J., Maita, S. and Nakatake, K. (1995), "A Simple Surface Panel Method to Predict Steady Marine Propeller Performance," Journal of the Society of Naval Architects of Japan, 178, 61-69.

Hess, J. L. and Smith, A.M.O. (2011), "Calculation of Nonlifting Potential Flow about Arbitrary Three

Dimensional Bodies," Journal of Ship Research, 8(2), 22-44.

Lan, C. E. (1974), "A Quasi-Vortex-attice Method in Thin Wing Theory," Journal of Aircraft, 11(9), 518-527.

Inukai, Y. (2011), "Development of Electric Propulsion Vessels with Contra-Rotating Propeller," Journal of the Japan Institution of Marine Engineering, 46(3), 313-319.

Inukai, Y., Kanemaru, T. and Ando, J. (2014), "Prediction of Steady Performance of Contra-Rotating Propellers Including Wake Alignment," Proc. of 11th International Conference on Hydrodynamics, Singapore.

ITTC. (2008), "The Specialist Committee on Azimuthing Podded Propulsion, Report and Recommendations to the 25th ITTC," Proc. of 25th ITTC, Japan.

Moriyama, F and Yamazaki, R. (1981). "On the Forces Acting on Rudder in Propeller Slip stream," Transaction of the West Japan Society of Naval Architects, 62, 23-40.

Nishiyama, S., Okamoto, Y., Ishida, S., Fujino, R., and Oshima, M. (1990). "Development of Contra Rotating Propeller System for JUNO a 37,000DWT Class Bulk-Carrier," Transaction of Society of Naval Architects and Marine Engineers, 98, 27-52.

Sasaki, N. (1990). "Study on Contrarotating Propellers," PH.D. Thesis, Kyushu University, Japan

DISCUSSION

Question from Ki-Han Kim

Your open water testing setup is not really open water due to the upstream strut and dynameter housing. How do you acocount for the effect of upsteam disturbunce in your open water performance?

Authors' Closure

Thank you for your question. We carried out open water test not only in the setup shown in Figure 4 but also in the normal setup which the propeller works in open water. By comparing the J-KT curves in both setups, we assumed that the wake of the upstream strut and dynameter housing is 8% of the undisturbed upstream flow speed. The advance ratio J in Figure 5 and 6 is normalized by the reduced advance speed due to the wake. Figure I shows that J-KT curves before and after the correction of J.

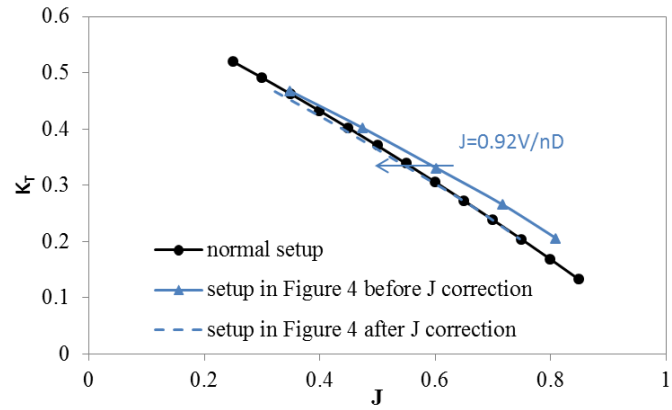

Figure I : J-KT curves before and after the correction of J.

Question from Kourosh Koushan

Please explain validity of your method for low advance ratio region 0-0.4.

Authors' Closure

Thank you for your question. We didn't carry out tests for the CRP in Table 1 at low J. Alternatively Figure II shows open water characteristics without a rudder for another CRP II in Table I which was carried out at low J in the Japan Marine United Yokohama towing tank. It is found that calculated K_T and K_Q of the aft propeller at low J is underestimated compared to the experiment. As shown in Figure III, the trailing wake of the forward propeller contracts largely due to the heavy load and the tip of the aft propeller is out of the slipstream of the forward propeller. The complicated interaction around the tip of the aft propeller with the trailing wake of the forward propeller can lead to the estimation error. We need more improvement of the wake model for heavily loading condition.

Table I: Principal dimensions of propellers.

	CRP II	
Diameter (m)	0.25	0.2083
Pitch Ratio	0.76	0.978
Number of Blades	4	5
Boss Ratio	0.18	0.216
Propeller revolution ratio of forward propeller to aft propeller nf/na	1.1	
Reynolds' Number (Kempf)	3.0×10^5	

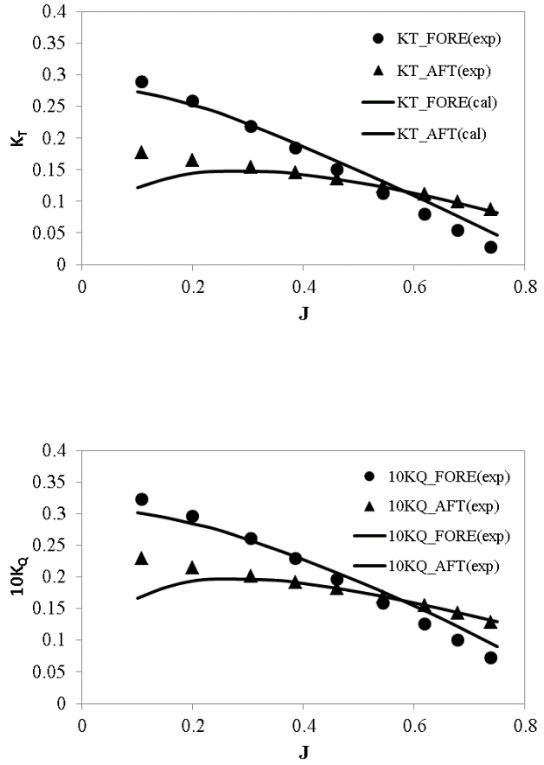

Figure II: Open water characteristics of CRP II.

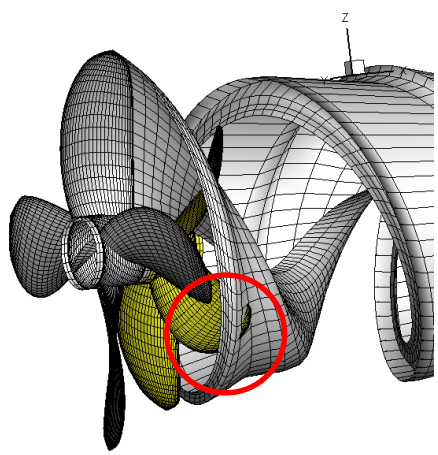

Figure III: Panels of trailing wake and surfaces of CRP II at J=0.2